

Controlling the Electronic Interaction between a Molecular Wire and Its Atomic Scale Contacting Pad

Leonhard Grill,* Karl-Heinz Rieder, and Francesca Moresco

*Institut für Experimentalphysik, Freie Universität Berlin, Arnimallee 14,
14195 Berlin, Germany*

Sladjana Stojkovic, André Gourdon, and Christian Joachim

*Nanoscience Group, CEMES–CNRS, 29 rue J.Marvig, P.O. Box 4347,
31055 Toulouse, France*

Received January 31, 2005

ABSTRACT

We report a quantitative study on the electronic interaction between a molecular wire and its atomic scale metallic contacting pad. A so-called “reactive Lander” molecule is manipulated using a low-temperature scanning tunneling microscope to form a planar one-end electronic contact. The increase of the STM contrast at the junction location is discussed by means of the electronic interaction between the contacting group of the molecular wire and the end atoms of the nanopad.

For the future development of molecular electronics, it is crucial to master quantitatively, at the atomic scale and in a planar configuration, the electronic contact between a single molecule and metallic electrodes, making possible the formation of well-defined molecular devices.^{1,2} Imaging the molecule–metal junction in the device with atomic scale precision^{3–5} is also becoming very important to allow the precise measurement of its length dependence conductance and of its corresponding contact conductance.²

More precisely, a well-defined planar electronic contact between a molecular wire and a metallic nanoelectrode requires (1) an atomically clean and structured contact pad having the suitable dimensions to fit the geometry of the end part of the molecular wire; (2) the decoupling of the molecular wire core from the metallic substrate to preserve the electronic integrity of the molecular wire; and (3) a specific contacting group at each end of the molecular wire whose chemical composition ensures a large electronic interaction with the nanopads.

Low temperature scanning tunneling microscopy (LT-STM) is a very useful technique to image the surface of a nanoelectrode with atomic precision before building the contact, to manipulate the molecule performing the contact, and to measure the tunneling current at the contact location when the contact is established. Lander and Cu(II) phthalocyanine

molecules have been recently manipulated by LT-STM to establish an electronic interaction between one end of the molecule and a metallic atomic scale structure or a monatomic step edge.^{3–5} In the corresponding LT-STM images, a small contrast increase was observed at the exact location of the molecule–metal junction. This was interpreted as a signature of a specific electronic interaction between the end of the molecule and the metallic pad.^{3,5}

After succeeding, as described in ref 5, in building molecule–metal electronic contacts according to requirements (1) and (2), we present in this letter the first report on the optimization of the contact end group of a molecular wire, respecting also (1) and (2). To improve the electronic interaction between the molecular wire end and its metallic nanopad, we have designed a new molecular wire where the weight of the π -molecular orbitals at both ends of the wire is increased by adding a double bond chemical group. In accordance with (2), semirigid legs are still attached sideways on the molecular wire, to decouple it electronically from the metallic surface underneath.⁶ The result is a new molecule called reactive Lander (RL), shown in Figure 1a. It consists of four lateral spacer legs (3,5-di-*tert*-butyl-phenyl groups) and a central board molecular wire. This board is longer than for a single Lander (SL)⁵ as it is elongated at both ends by the described double bonds.

Experiments were performed by LT-STM in an ultrahigh-vacuum chamber with a base pressure of 10^{-10} mbar. Small amounts of RL molecules (about 0.01 monolayer) were

* Corresponding author. Phone: +49 (0)30 8385 4575 (6039). Fax: +49 (0)30 8385 1355. E-mail: leonhard.grill@physik.fu-berlin.de.

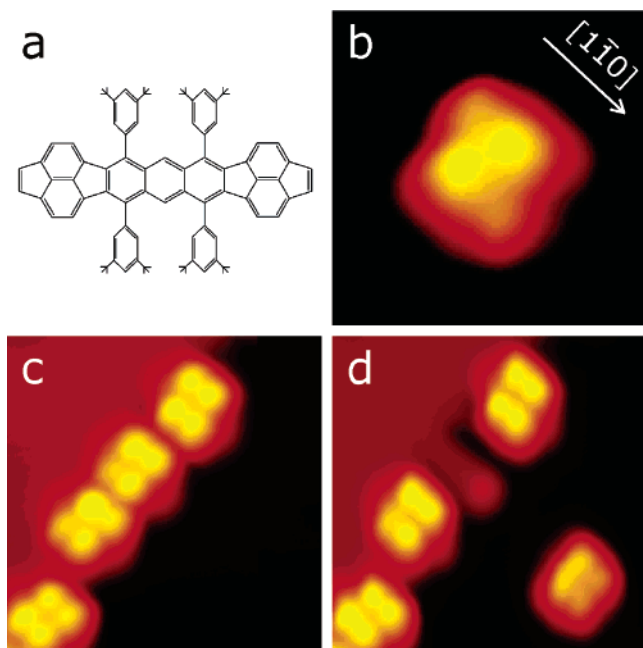


Figure 1. (a) Chemical structure of the RL molecule. (b) RL molecule on a Cu(110) terrace after removal from a step edge by lateral manipulation ($40 \times 40 \text{ \AA}^2$). The substrate orientation $[1\bar{1}0]$ is indicated and is the same for all STM images. (c) RL molecules adsorbed at a Cu(110) step edge ($80 \times 80 \text{ \AA}^2$). (d) After removal of a molecule by lateral manipulation a nanopad is visible at the adsorption site while the intact molecule is on the lower terrace ($80 \times 80 \text{ \AA}^2$).

deposited at room temperature on the surface of a Cu(110) sample, which has been cleaned before by Ne ion sputtering and subsequent annealing at 770 K. The temperature of the molecule evaporator, a Knudsen cell, was about 620 K as controlled by a thermocouple. STM images were taken in constant-current mode at temperatures between 7 and 8 K with a home-built LT-STM,⁷ capable of atomic and molecular manipulation.^{8,9} Bias voltages between 0.3 and 0.5 V (with respect to the tip) and tunneling currents between 0.3 and 0.6 nA were used.

The atomic scale metallic nano-pads were fabricated by the molecules themselves. In this respect, we benefit from the known ability of the Lander molecules to restructure the Cu(110) substrate at monatomic step edges.^{5,10} A Cu atomic wire, two atoms wide and in average seven atoms long, is formed under each Lander molecule and provides the atomic scale nanopad for our planar contacting experiments. To facilitate the formation of such Cu nanostructures, the sample was annealed to 370 K after the deposition of the molecules. Once the nanopad is formed, the temperature is lowered to about 7 K and the molecule can be removed from the step edge (Figure 1c) by lateral manipulation^{8,9} onto the terrace. A tooth-like Cu nanostructure is easily found at the position where a RL molecule was previously located (Figure 1d).

Along one of these self-fabricated nanopads, a RL molecule can be found in various different conformations. Before discussing them, it should be recalled that STM images of molecules of the Lander series on a flat terrace are dominated by the molecular legs, while the central board is not visible.^{3,5,10–13} This is also the case for the new RL

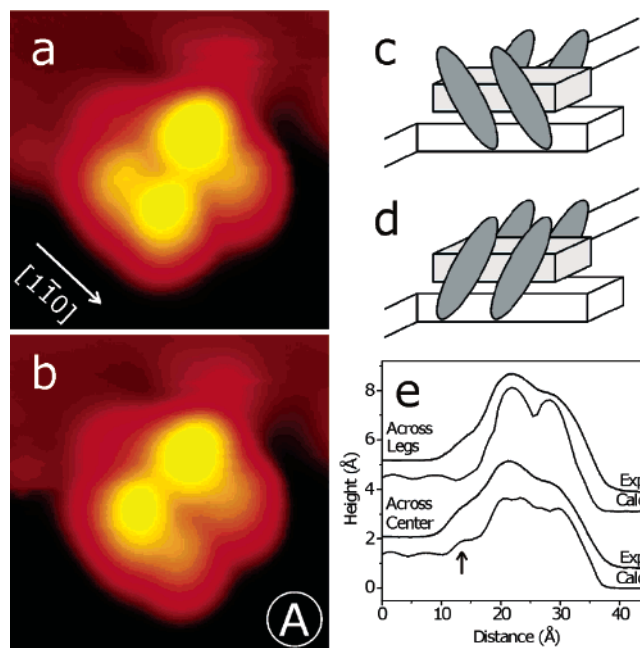


Figure 2. (a) STM image of a RL molecule in the crossed-legs and (b) in the parallel-legs conformation on the copper nanopad (both $35 \times 35 \text{ \AA}^2$). (c) Schematic view of the crossed-legs and (d) of the parallel-legs conformation. (e) Comparison of experimental (exp) and calculated (calc) line scans across board and legs in $[1\bar{1}0]$ direction for the parallel-legs conformation in b. The arrow marks the position where additional intensity due to an electronic interaction contributes to the STM image.

molecules.¹⁴ On a Cu(110) terrace, RL molecules are found in a characteristic crossed-legs conformation (Figure 1b) and also in a parallel-legs conformation (Figure 1d). Along its nanopad, RL is mostly found in the parallel-legs conformation (as already observed for the SL⁵). However, the crossed-legs (Figure 2a) and a second parallel-legs conformation (Figure 2b, schematically shown in Figure 2c and d respectively), where all legs are rotated toward the lower terrace, can also be achieved by manipulation with the STM tip. A further interesting molecular conformation is reached when an RL molecule is manipulated up to the end of its nanopad (Figure 3a). In this case, the end group of the molecular wire is interacting with the nanopad. It is, however, important to note that in this case the geometry of the contact is not planar as the molecular wire is slightly tilted over the nanopad (schematically shown in Figure 3b).

To reach the planar contact configuration (called configuration C in the following), an RL molecule is first manipulated from its nanopad onto the lower terrace. Then, it is manipulated back toward the end of the nanopad (Figure 3d). In this way, a planar “molecule–nanopad” junction is created, where the four legs of the RL molecule are still remaining on the lower terrace. As shown schematically in Figure 3e, the double bond at one end of the molecular wire is now interacting with the end atoms of the nanopad while the RL molecular board is kept planar. Notice that such planar contact configuration cannot be obtained with the SL molecule because the board is too short, so that the front legs maintain the board end too far away from the nanopad end.

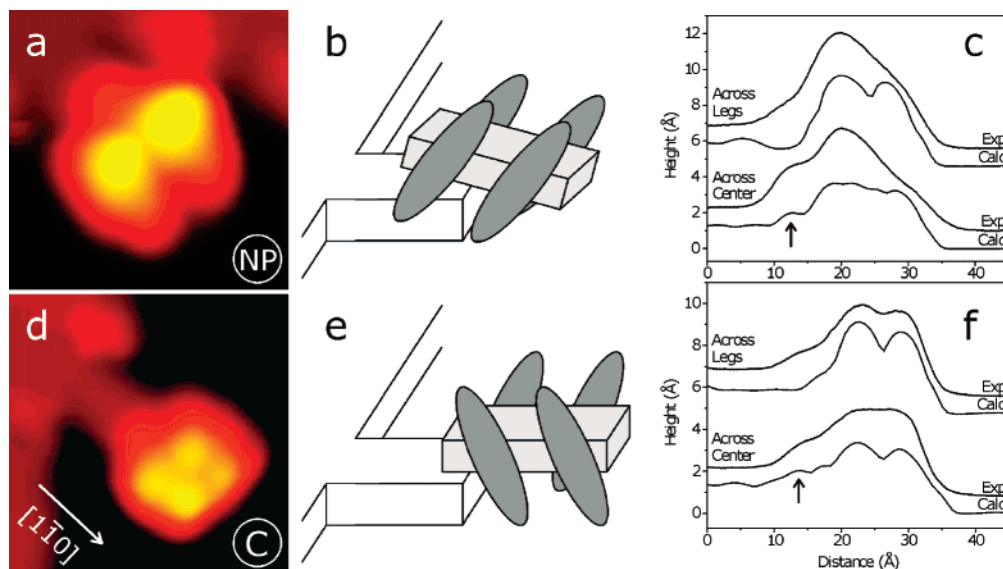


Figure 3. Upper panel: RL in non planar conformation (called conformation NP in the text). (a) STM image ($35 \times 35 \text{ Å}^2$), (b) schematic view, and (c) height profiles across a pair of legs and across the center of the molecule in $[1\bar{1}0]$ direction as taken from experimental (exp) and calculated (calc) images. Lower panel: RL in planar contact conformation with the nanopad (called conformation C in the text). (d) STM image ($45 \times 45 \text{ Å}^2$), (e) schematic view, and (f) height profiles as in (c). The arrows mark the position where additional intensity due to an electronic interaction contributes to the STM image.

With the RL contacted to the nanopad in the planar configuration C, the signature of an electronic interaction between the end group of the RL molecular wire and the end atoms of the nanopad is clearly observed at the location of the molecular wire double bond. In two other RL configurations, an enhanced STM contrast can be also observed at this location. The first one corresponds to the entire RL molecule positioned on the nanopad with the board flat and a parallel-legs configuration (adsorption configuration, called A, defined in Figure 2b, d, and e). In the second one, the RL molecule is positioned at the end of the nanopad with a tilted central board (nonplanar configuration NP, Figure 3a–c).

For a quantitative description of the electronic interaction, we extract the increase of the STM apparent height Δh at the end board location from line scans in the $[1\bar{1}0]$ direction across the center of the molecule. A background caused by the molecular legs is subtracted, to consider exclusively the contrast due to the end part of the board. For the contact configuration C, we obtain a value of $\Delta h = 0.53 \pm 0.03 \text{ Å}$, while configuration A shows a $\Delta h = 0.37 \pm 0.03 \text{ Å}$. A larger value of Δh is obtained for the nonplanar case (configuration NP), where $\Delta h = 0.68 \pm 0.05 \text{ Å}$. Notice that in the case of a SL molecule, an enhanced contrast was visible in the STM images at the end location of the molecular wire only for the nonplanar configuration⁵ with a relatively small contribution $\Delta h = 0.22 \pm 0.07 \text{ Å}$. This confirms the optimization performed on the chemical structure of the end group of our molecular wire, which largely favors the electronic interaction between the molecular wire and the end atoms of the nanopad, compared to the chemical structure of the SL molecular wire end.

To analyze the observed Δh variations, we have first determined the effective conformation of the RL molecule and its adsorption position in the different configurations A,

NP, and C by performing a molecular conformation refinement using a molecular mechanics–electron scattering quantum chemistry (MM-ESQC) method.¹⁵ Experimental line scans recorded both across the RL legs and across the board are compared with the ESQC calculated ones, obtained after a molecular mechanics optimization of the RL physisorbed on the copper surface. The reported experimental results for the RL molecules are well reproduced by the calculated line scans: $\Delta h = 0.5 \text{ Å}$ for A, $\Delta h = 0.75 \text{ Å}$ for NP, and $\Delta h = 0.6 \text{ Å}$ for C. In the case of a calculated line scan, the background caused by the legs is more precisely evaluated than in the experiment by calculating a separate curve where only the molecular orbitals of the legs (and no central board) are taken into account. The calculated Δh values are slightly larger than the experimental ones as the real tip apex is presumably broader than the one assumed in the calculations. However, the qualitative differences among the three values are equivalent. Calculated and experimental line scans along the $[1\bar{1}0]$ direction for the cases A, NP, and C are compared in Figure 2e, 3c, and 3f, respectively.

The observed Δh is the remaining part of the STM contrast that the board of the RL would provide if adsorbed alone (without the legs) on the Cu(110) surface in the same adsorption geometry. The Δh amplitude is a measure of the electronic interaction between the contact end group and the metallic pad.^{3,5} Therefore, to understand the differences between the Δh values, we have calculated in Figure 4 how the STM contrast produced by the terminal double bond of the RL board alone depends on the distance z of the board from the Cu(110) surface and on the board adsorption site. No legs were considered in order to avoid their dominating role in the STM contrast (see Figures 2 and 3). The studied adsorption configurations are shown schematically in the upper panel of Figure 4.

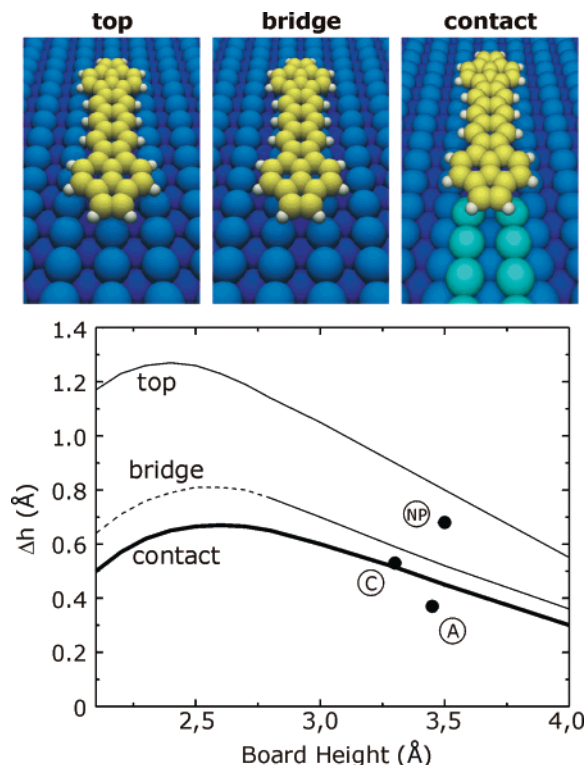


Figure 4. Upper panel: Sphere models of the bare central board (oriented in the $[110]$ direction) in the top, bridge, and contact adsorption positions with respect to the Cu(110) surface. Lower panel: STM apparent height Δh at the end board location as a function of the distance of the molecular board from the surface. Solid lines represent calculations whereas circles indicate experimental results for three different conformations: RL in planar contact with the nanopad (C); RL with parallel legs rotated toward the lower terrace (A); RL in "nonplanar" conformation (NP). At small board heights (below 2.7 Å), the bridge site adsorption curve is estimated (dashed line) as the contact bump from the double bond is overshadowed by contributions from other molecular orbitals.

Assuming top site adsorption on a Cu(110) terrace (uppermost curve in Figure 4), the STM maximum corrugation at the double bond location is $\Delta h = 1.3$ Å for a board height of $z \approx 2.5$ Å. This adsorption geometry is reasonable for the bare RL board as it is equivalent to that of the isoelectronic pentacene molecule on Cu(110).¹⁶ According to this top site Δh curve, a smaller Δh value is found for the chemisorption distance of the board (about 2.3 Å). This is due to the large mixing of the electronic states of the surface with the molecular levels that changes the local density of states at the surface, increasing the apparent tunneling barrier height.

If a bridge site adsorption geometry is assumed (central curve in Figure 4), the maximum of $\Delta h(z)$ is 0.8 Å for a board height of $z \approx 2.6$ Å. This new adsorption site was selected considering that, when the legs are present, the RL board is constrained to remain in the center of the nanopad, i.e., in bridge site adsorption geometry. In this case, the double bond end group corrugation is clearly smaller than for a top site because the terminal double bond is not centered at the position of a surface copper atom.

According to this bridge site curve, one expects a Δh maximum for configuration C. In this case, the distance between the board and the surface (3.8 Å on the bare terrace as maintained by the legs) will be reduced by the step height (1.27 Å) at the location of the junction between the RL board and the end atoms of the nanopad. From this simple estimation we would obtain a distance of 2.5 Å, which corresponds to a maximum in Δh of about 0.8 Å for the bridge site.

Therefore, we have calculated the corresponding $\Delta h(z)$ curve for a contact formed by a RL board positioned at the end of a nanopad made of two copper atomic rows on Cu(110) (see Figure 4 contact configuration). This case is reflected by the lowermost curve in Figure 4 (contact curve). It turns out that the Δh maximum is only 0.65 Å (and not 0.8 Å as evaluated from the simple geometrical reasoning above) if the board is considered rigid and 2.5 Å above the nanopad end. However, the board is not rigid¹¹ as a conformation refinement shows that the legs are deformed in contact configuration C. The resulting board height $z = 3.3$ Å corresponds to a calculated value of $\Delta h = 0.52$ Å on the lowermost curve in Figure 4.

In Figure 4, these theoretical results are compared with the three experimental Δh values already discussed for configurations A, NP, and C (presented in Figures 2 and 3). As can be seen, the data point corresponding to the contact configuration C ($\Delta h = 0.53 \pm 0.03$ Å) is in perfect agreement with the calculations (exactly on the contact curve). The relatively large value of the nonplanar configuration (NP) is probably due to the electronic interaction not only of the double bond end but also of the central part of the molecular wire with the end of the nanopad (see scheme in Figure 3b). Finally, configuration A gives an experimental value of $\Delta h = 0.37 \pm 0.03$ Å, quite close to the calculated 0.45 Å.

In conclusion, we have investigated with a LT-STM the electronic interaction between the double bond end group of a molecular wire when contacted to an atomic scale nanopad. A planar contact configuration is obtained when the RL molecule is connected by STM manipulation to the end of the nanopad. The corresponding increase of the STM contrast at the contact location is very close to the theoretically predicted value considering an electronic interaction between the end of the molecular wire and the terminal atoms of the nanopad. By studying the STM contrast in detail and comparing the contacted case with other adsorption geometries of the RL molecule on the nanopad, we demonstrate that the observed electronic interaction depends on a very delicate balance between the chemisorption site, the height of the chemical group forming the contact, and the kind of electronic states existing at the end of the contacting pad. The new double bond contacting group is working better than the simple naphthalene group at the end of the molecular wire and represents a further step to achieve a large contact conductance at a molecule–nanopad junction.

References

- (1) Smit, R. H. M.; Noat, Y.; Untiedt, C.; Lang, N. D.; van Hemert, M. C.; van Ruitenbeek, J. M. *Nature* **2002**, *419*, 906.

- (2) Joachim, C.; Gimzewski, J. K.; Aviram, A. *Nature (London)* **2000**, 408, 541.
- (3) Moresco, F.; Gross, L.; Alemani, M.; Rieder, K.-H.; Tang, H.; Gourdon, A.; Joachim, C. *Phys. Rev. Lett.* **2003**, 91, 036601.
- (4) Nazin, G. V.; Qiu, X. H.; Ho, W. *Science* **2003**, 302, 77.
- (5) Grill, L.; Moresco, F.; Jiang, P.; Joachim, C.; Gourdon, A.; Rieder, K.-H. *Phys. Rev. B* **2004**, 69, 035416.
- (6) Gourdon, A. *Eur. J. Org. Chem.* **1998**, 2797, 7.
- (7) Meyer, G. *Rev. Sci. Instrum.* **1996**, 67, 2960.
- (8) Strosio, J. A.; Eigler, D. M. *Science* **1991**, 254, 1319.
- (9) Bartels, L.; Meyer, G.; Rieder, K.-H. *Phys. Rev. Lett.* **1997**, 79, 697.
- (10) Rosei, F.; Schunack, M.; Jiang, P.; Gourdon, A.; Laegsgaard, E.; Stensgaard, I.; Joachim, C.; Besenbacher, F. *Science* **2002**, 296, 328.
- (11) Zambelli, T.; Tang, H.; Lagoute, J.; Gauthier, S.; Gourdon, A.; Joachim, C. *Chem. Phys. Lett.* **2001**, 348, 1.
- (12) Kuntze, J.; Berndt, R.; Jiang, P.; Tang, H.; Gourdon, A.; Joachim, C. *Phys. Rev. B* **2002**, 65, 233405.
- (13) Gross, L.; Moresco, F.; Alemani, M.; Tang, H.; Gourdon, A.; Joachim, C.; Rieder, K.-H. *Chem. Phys. Lett.* **2003**, 371, 750.
- (14) Gross, L.; Moresco, F.; Savio, L.; Gourdon, A.; Joachim, C.; Rieder, K.-H. *Phys. Rev. Lett.* **2004**, 93, 056103.
- (15) Sautet, P.; Joachim, C. *Chem. Phys. Lett.* **1991**, 185, 23.
- (16) Lukas, S.; Witte, G.; Wöll, Ch. *Phys. Rev. Lett.* **2002**, 88, 028301.

NL050197Z